Available online at www.sciencedirect.com
SCIENCE DIRECT®
Vision Research 44 (2004) 3297–3306
Vision Research
www.elsevier.com/locate/visres

Function and plasticity of homologous coupling between AII amacrine cells

Stewart A. Bloomfield *, Béla Völgyi

Departments of Ophthalmology and Physiology and Neuroscience, New York University School of Medicine, 550 First Avenue, New York, NY 10016, USA

Received 5 May 2004; received in revised form 19 July 2004

Abstract

The AII amacrine cells are critical elements in the primary rod pathway of the mammalian retina, acting as an obligatory conduit of rod signals to both on- and off-center ganglion cells. In addition to the chemical synaptic circuitry they subserve, AII cells form two types of electrical synapses corresponding to gap junctions formed between neighboring AII cells as well as junctions formed between AII cells and on-center cone bipolar cells. Our recent results indicate that coupling between AII cells and cone bipolar cells forms an obligatory synapse for transmission of scotopic visual signals to on-center ganglion cells. In contrast, AII–AII cell coupling acts to maintain the sensitivity of the primary rod pathway by allowing for summation of synchronous activity and the attenuation of asynchronous background noise. Further, the conductance of AII–AII cell gap junctions is highly dynamic, regulated by ambient light conditions, thereby preserving the fidelity of rod signaling over the scotopic operating range from starlight to twilight.

1. Introduction

In the mammalian retina, rod and cone photoreceptors synapse onto largely different bipolar cells, thereby segregating their signals into different vertical streams (Boycott & Dowling, 1969; Boycott & Kolb, 1973). Whereas up to 11 different morphological types of cone bipolar have been reported, showing both on- and off-center physiology, only a single type of rod bipolar cell exists (Boycott & Wässle, 1991; Euler & Wässle, 1995). Interestingly, the axons of rod bipolar cells do not directly contact ganglion cells, but, instead, contact mainly the small-field, bistratified AII amacrine cell (Kolb, 1977; Strettoi, Dacheux, & Raviola, 1990). In turn, AII cells form sign-conserving electrical synapses with the axon terminals of on-center cone bipolar cells and sign-inverting glycinergic chemical synapses with the axon terminals of off-center cone bipolar cells (Strettoi, Dacheux, & Raviola, 1992). In this way, both on- and off-center scotopic signals utilize the cone pathways before reaching the ganglion cells and ultimately higher brain centers.

An alternative or secondary rod pathway has been suggested by the gap junctions formed between the terminals of rod and cone photoreceptors (Raviola & Gilula, 1973). In this scheme, rod signals flow directly into cones and then use cone bipolar cells to reach the ganglion cells. Evidence for the operation of this secondary pathway includes the finding of rod signals in cone photoreceptors (Nelson, 1977; Schneeweis & Schnapf, 1995), axonless horizontal cells (Bloomfield & Miller, 1982; Dacheux & Raviola, 1982; Nelson, 1977), and different scotopic thresholds of rod and cone bipolar cells (Field & Rieke, 2002). Further, both physiological and psychophysical evidence now support the existence of two rod pathways, suggesting that the primary rod bipolar-AII cell pathway carries a high-sensitivity rod signals

* Corresponding author. Tel.: +1 212 263 5770; fax: +1 212 263 8072.
E-mail address: blooms01@med.nyu.edu (S.A. Bloomfield).

0042-6989/$ - see front matter © 2004 Elsevier Ltd. All rights reserved.
doi:10.1016/j.visres.2004.07.012

with the secondary pathway transmitting less sensitive rod signals (Deans, Völgyi, Goodenough, Bloomfield, & Paul, 2002; Sharpe & Stockman, 1999). Consistent with the well-described circuitry, recent work in our lab using a connexin36 (Cx36) knockout mouse, in which the AII cell-to-cone bipolar cell and rod–cone gap junctions are eliminated, showed unequivocally that these gap junctions form obligatory synapses for the transmission of rod signals within the two rod pathways (Deans et al., 2002). These results also suggested that signals carried by the primary rod pathway are, indeed, about one log unit more sensitive than those carried by the secondary pathway.

In addition, it is well known that neighboring AII cells are also extensively coupled to each other suggesting an electrical syncytium within the inner retina. Unfortunately, the underlying circuitry provides no hint as to the function of this homologous coupling between AII cells (Famiglietti & Kolb, 1975; Strettoi et al., 1992; Vaney, 1991). Although computational studies indicate that AII–AII cell coupling improves signal-to-noise properties of their responses (Smith & Vardi, 1995), its overall function remains unclear. In this report, we summarize recent studies in our laboratory showing that the AII–AII cell coupling is highly dynamic, being modulated by changes in adaptational state. Moreover, elimination of this coupling in the Cx36 knockout mouse results in an approximate one log unit loss in the response threshold of postsynaptic ganglion cells. Overall, our recent results indicate that AII–AII cell coupling preserves the high sensitivity of signals carried to the inner retina via the primary rod pathway.

2. Methods

2.1. Preparation

The general methods used in this study have been described previously (Bloomfield & Miller, 1982; Bloomfield, Xin, & Osborne, 1997; Deans et al., 2002). Procedures were in accordance with the guidelines of the National Institutes of Health and the Institutional Animal Care Committee at NYU School of Medicine. For mice experiments, adult (P_{42-90}) wild-type and Cx36 knockout mice (Deans, Gibson, Sellitto, Connors, & Paul, 2001) were used for both tracer injections and electrophysiological recordings. The mice were deeply anesthetized with an intraperitoneal injection of Nembutal (0.08 g/g body-weight). Lidocaine hydrochloride (20 mg/ml) was applied locally to the eyelids and surrounding tissue. For rabbit experiments, adult, Dutch-belted rabbits (1.5–3.0 kg) were anesthetized with an intraperitoneal injection of ethyl carbamate (2.0 g/kg) and a local injection of 2% lidocaine hydrochloride into the tissue surrounding the eyelids. A flattened retinal-scleral preparation developed for rabbit by Hu, Dacheux, and Bloomfield (2000) was adopted and modified for the mouse as well. Briefly, the eye was removed under dim red illumination and hemisected anterior to the ora serrata. Anterior optics and the vitreous humor were removed and the resultant retina-eyecup was placed in a superfusion chamber. Several radial incisions were made peripherally allowing the eyecup to be flattened. The chamber was then mounted in a light-tight Faraday cage and superfused with oxygenated mammalian Ringer solution (pH = 7.4, 32 °C) (Bloomfield & Miller, 1982). Following enucleations, animals were killed immediately by either cervical dislocation (mice) or an intracardial bolus injection of ethyl carbamate (rabbits).

2.2. Light stimulation

For extracellular recordings, a green ($\lambda = 468$ nm) light emitting diode delivered uniform fullfield visual stimuli on the surface of the retina. The intensity of the square wave light stimuli was calibrated with a portable radiometer/photometer (Ealing Electro-Optics, Inc., Holliston, MA) and expressed in terms of the time-average rate of photoisomerizations per rod per second (Rh^*/rod/s). Light intensities were calculated assuming an average rod density of 437,000 rods/mm^2 (Jeon, Strettoi, & Masland, 1998) and quantum efficiency of 0.67 (Penn & Williams, 1984). The intensity of the light stimuli varied from 10^{-2} to 10^4 Rh^*/rod/s. In addition, two 100 W quartz-iodide lamps provided white light for a dual beam optical bench. Light intensity could be reduced up to 7 log units with calibrated neutral density filters placed in the light path of both beams. The maximum irradiance of both beams was equalized at 2.37 mW/cm^2. The beams were combined with a collecting prism and focused onto the vitreal surface of the retina-eyecup by means of a final focusing lens. The bottom beam provided small concentric spot stimuli (50 μm to 6.0 mm diameter) as well as a 50 μm wide/6.0 mm long rectangular slit of light which was moved along its minor axis (parallel to the visual streak) in steps as small as 3 μm. Alignment of the electrode tip with stimuli was accomplished visually with the aid of a dissecting microscope mounted in the Faraday cage. However, after impaling a cell, the spot stimulus which evoked the largest amplitude center-mediated response was considered centered over the cell and adjustment of stimuli position was made accordingly. All retinas were left in complete darkness for at least 45 min prior to recording. In the search for cells, light stimuli of log −6.0 or log −5.5 intensity (approximately 1 log unit above rod threshold) were presented only once every 10 s to limit any light adaptation.

2.3. Electrical recordings

Extracellular recordings were then obtained from ganglion cells using insulated tungsten microelectrodes with resistances of 0.9–1.2 MΩ (Micro Probe, Inc., Potomac, MD). Spike trains were recorded digitally at a sampling rate of 20 kHz with Axoscope (Axon Instruments, Inc., Foster City, CA). For further off-line analysis, Offline Sorter (Plexon Inc., Dallas, TX) and Nex (Nex Technologies, Littleton, MA) software were used. Intensity–response profiles for individual cells were generated by tabulating spike counts in 500 ms bins before, during and after presentation of a 500 ms duration stimulus with intensities varied over 6 log units. Numbers of light-evoked ON and OFF spikes of ganglion cells were calculated by a subtraction of the background spike activity from those evoked by the light stimulus onset and offset, respectively. Averaged response data were then normalized and plotted against the intensity of the light stimuli using Origin software (Microcal Software, Inc., Northampton, MA). Data points were fitted by the classic Michaelis–Menten equation (cf. Baylor, Hodkin, & Lamb, 1974; Naka & Rushton, 1966; Thibos & Werblin, 1978):

$$R = \frac{R_{\max} I^a}{I^a + \sigma^a}$$

where R = measured response, $R_{\max}$ = maximum response, I = stimulus intensity, σ = light intensity that produces response of $0.5R_{\max}$ and a = Hill coefficient.

Intracellular recordings were obtained with microelectrodes fashioned from standard borosilicate glass tubing (Sutter Instruments). Electrodes were filled at their tips with 4% *N*-(2-amino-ethyl)-biotinamide hydrochloride, Neurobiotin (Vector Laboratories), in 0.1 M Tris buffer (pH 7.6) and then back filled with 4 M potassium chloride. Final dc resistances of electrodes ranged from 250 to 450 MΩ. Following physiological characterization of a cell, Neurobiotin was iontophoresed into the neuron using a combination of sinusoidal (3 Hz, 0.8 nA p–p) and dc current (0.4 nA) applied simultaneously; this method allowed passage of tracer through the electrode without polarization. Recordings were displayed on an oscilloscope, recorded on magnetic tape, and digitized off-line for computer analyses. For pharmacological studies, drugs were applied by switching from the control solution described above to one containing a known concentration of drug.

2.4. Histology

One hour after labeling the last cell in an experiment, the retina was fixed in a cold (4 °C) solution of 4% paraformaldehyde–0.1% glutaraldehyde in 0.1 M phosphate buffer (pH 7.3) for 12 min. The retina was then detached, trimmed, and fixed onto a gelatinized glass coverslip and left in fixative overnight at 4 °C. Retinas were then washed in phosphate buffer and reacted with the Elite ABC kit (Vector Laboratories) and 1% Triton X-100 in 10 mM sodium phosphate-buffered saline (9% saline, pH 7.6). Retinas were subsequently processed for peroxidase histochemistry using 3,3′-diaminobenzidine (DAB) with cobalt intensification. Retinas were then dehydrated, cleared, and flatmounted for light microscopy.

3. Results

3.1. Light-induced modulation of AII amacrine cell coupling

In the dark-adapted retina, AII amacrine cells display a stereotypic on-center/off-surround receptive field organization (Fig. 1A and B). The light-evoked response consists of a transient depolarization at light onset followed by a sustained component and a large, oscillating hyperpolarization. The initial transient is composed of superimposed smooth and oscillatory waves; the latter may reflect intrinsic sodium or calcium conductances (Dacheux & Raviola, 1986). Peripheral stimulation evokes a prominent surround-mediated response consisting of a sustained hyperpolarization and often an oscillatory depolarizing response at light offset. On rare occasions, AII cells show sodium-mediated spike activity (Bloomfield & Xin, 2000; Boos, Schneider, & Wässle, 1993).

Dark-adapted AII cells show relatively small on-center receptive fields extending approximately 60–80 μm across and off-surround receptive fields extending 100–130 μm (Fig. 1C). The small receptive field of a dark-adapted AII cell is about twice the extent of its narrow dendritic arbor. This small difference would appear inconsistent with the fact that neighboring AII cells show numerous, prominent gap junctions suggesting far more extensive lateral signal propagation across the IPL. However, when the biotinylated tracer, Neurobiotin, is injected into a dark-adapted AII amacrine cell it typically labels only a small array of 7–10 darkly labeled AII cells surrounded by a more lightly-labeled array of 10–15 AII cells (Fig. 2A and C). A group of smaller cell bodies identified as cone bipolar cells are also visible, presumably labeled by tracer movement across the AII-cone bipolar cell gap junctions (Fig. 2D and E). These data indicate that, under dark-adapted conditions, AII amacrine cells are coupled in circumscribed arrays that corresponds well to the size of their individual on-center receptive fields. That is, the conductance of the AII–AII cell gap junctions effectively limits the movement of both ionic current and tracer molecules.

The situation differs dramatically when the retina is adapted with background illumination in which the

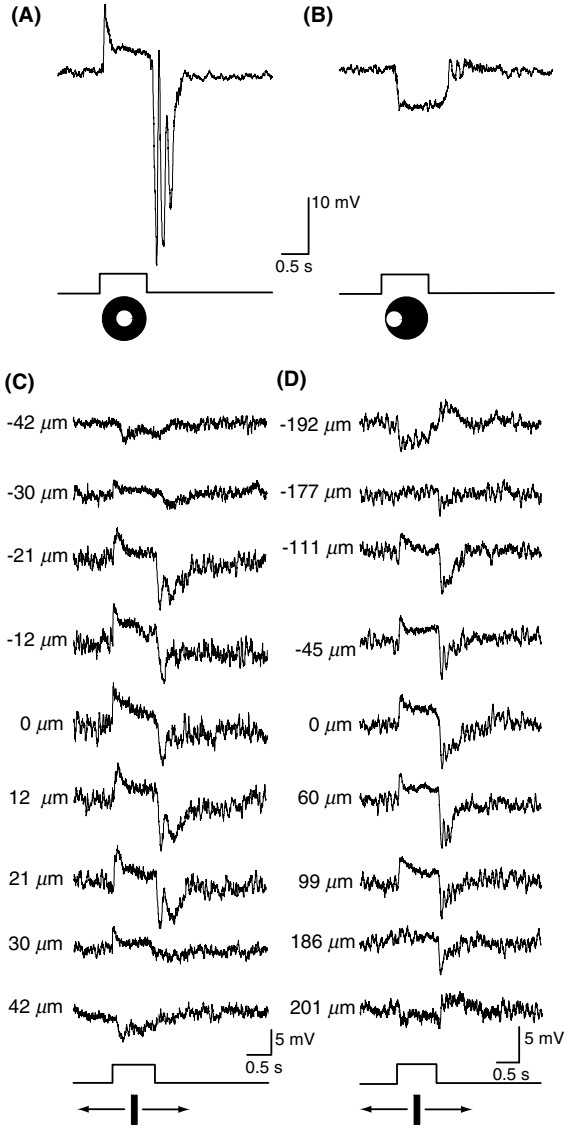

Fig. 1. (A) Typical response of a dark-adapted AII cell consisting of a transient at light onset, a sustained depolarization and a large oscillating hyperpolarization at light offset. Stimulus was a 75 μm diameter spot of light centered over the cell. Stimulus intensity = log −5.5. Trace below response indicates onset and offset of the light stimulus. (B) Response of same cell as in A after the small spot of light was translated laterally by about 100 μm. Translated spot evokes an off-surround response. (C) Light-evoked responses of an AII amacrine in a well dark-adapted retina. Stimulus is a 50 μm wide/6.0 mm long rectangular slit of light which was moved in discrete steps across the retinal surface. At 0 μm the slit was centered over the cell. The values to the left of each trace represent how far off-center the slit was positioned; polarity of number indicates direction of movement. Center receptive field is about 70 μm. Stimulus trace is presented at the bottom of the figure. Stimulus intensity = log −5.5. Maximum intensity (log 0.0) = 2.37 mW/cm^2. (D) Light-evoked responses of an AII amacrine in a retina maintained under constant background illumination of −5.5 log intensity. Stimulus is a 50 μm wide/6.0 mm long rectangular slit of light which was moved in discrete steps across the retinal surface. Conventions the same as in Fig. 1C. The center receptive field of this cell was measured at 399 μm along the axis parallel to the visual streak, considerably larger than that for the dark-adapted AII cell. Stimulus intensity = log −4.5. Maximum intensity (log 0.0) = 2.37 mW/cm^2.

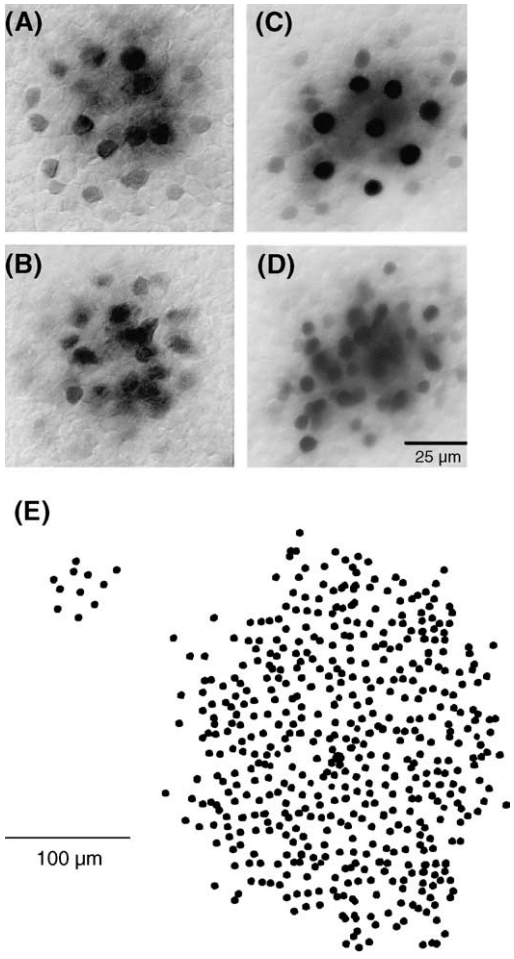

Fig. 2. Photomicrograph providing a flatmount-view of a group of tracer-coupled AII amacrine cells in mouse (A and B) and rabbit (C and D) following injection of one cell with Neurobiotin. Fullfield illumination for 1 h prior to the tracer injection. Plane of focus is on the AII cell somata in the proximal inner nuclear layer in A and C. (B and D) Plane of focus on on-center cone bipolar cell somata in the more distal inner nuclear layer were also labeled by the injection. (E) Schematic comparing the number of tracer-coupled AII cell somata following injection of a single AII cell in a well dark-adapted retina (left) and an AII cell adapted for 30 min with a constant dim background light of log −6.0 intensity.

neuromodulator dopamine, acting as a light-activated mediator (reviewed by Witkovsky & Dearry, 1992), alters the AII cell coupling (Hampson, Vaney, & Weiler, 1992). Fig. 1D shows the response profile of an AII cell under a constant adapting light of log −5.5 intensity, approximately 1.5 log units above rod threshold. Under these conditions, the response waveform remains quite similar to that seen in the dark-adapted retina. However, the on-center receptive field measures approximately 400 μm across, some 6–7 times the size of the center receptive fields of dark-adapted AII cells. Consistent with the increase in receptive fields seen for AII cells adapted with dim background lights, there is also a significant increase in the extent of tracer coupling following injection of Neurobiotin. For example, Fig. 2E

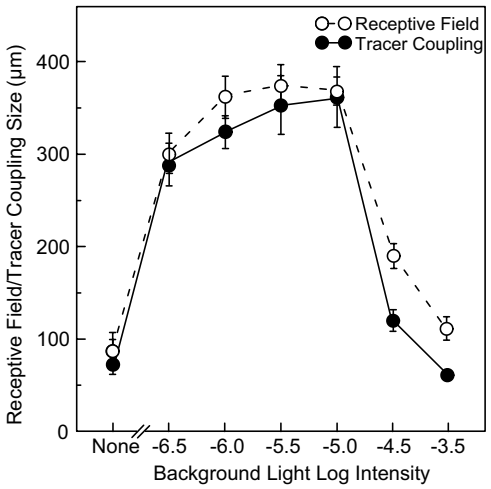

Fig. 3. Scatterplot comparing the tracer coupling and receptive field size of AII cells injected with Neurobiotin across a range of background light intensities corresponding to the scotopic and mesopic levels. Each data point illustrates the average and standard error of multiple injections. Well dark-adapted retinas are represented by data point corresponding to 'none' background light intensity. Note the inverted U-shaped function followed by both curves.

provides a schematic illustrating the coupling pattern of a dark-adapted AII amacrine cell after injected with Neurobiotin and another array formed when an AII cell is adapted with a very dim background light of log −6.0. Whereas the dark-adapted array is limited to just 11 AII cell somata, 443 coupled AII cells could be visualized following exposure to the dim background light.

Fig. 3 summarizes the change in tracer coupling pattern and receptive field size of AII cells seen under different adapting conditions. Whereas dark-adapted AII cells are coupled in relatively small groups and show relatively small receptive fields, exposure to dim background lights brings about an approximate 7-fold increase in the extent of both tracer coupling and receptive field size. The increased coupling between light-sensitized AII cells corresponds to a proportional increase in the size of their individual on-center receptive fields. Further light adaptation of the retina results in a decrease in coupling to levels similar to those seen in dark-adapted retina. These robust concomitant changes in tracer coupling and receptive field size of AII cells indicate a clear modulation of AII–AII cell coupling under different adaptational states. Under scotopic conditions, AII cells appear to have two main states of coupling; weak coupling under very dark-adapted conditions near rod threshold and relatively strong coupling under the remaining scotopic background light conditions.

3.2. Scotopic intensity–response functions of ganglion cells

The above data indicate that there is a concise relationship between the extent of AII cell coupling and the level of dark adaptation. Yet, they do not address the fundamental question: why are AII cells homologously coupled? To study this problem, we focused on the responses of the postsynaptic ganglion cells. Our strategy was to examine the intensity–response profiles of individual ganglion cells in the mouse retina under identical dark-adapted conditions. We found that ganglion cells could be placed into distinct groups based on their thresholds and intensity–response profiles (Deans et al., 2002). However, in this report, we will limit our analysis to two groups that we term high- and intermediate-sensitivity cells. Under scotopic conditions, both on- and off-center cells could be placed in the high- and intermediate-sensitivity groups, the former group showing an average threshold of approximately 0.04 Rh^*/rod/s and the latter group showing about one log unit less sensitivity. This division was also evident when the averaged, normalized intensity–response profiles were fitted with Michaelis–Menten functions (Fig. 4A and B).

The finding of two physiological groups of cell, based on their scotopic intensity–response functions, could reflect segregated input from the primary and secondary rod pathways. To test this hypothesis, we pharmacologically blocked the primary rod pathway. We used the nitric oxide donor, SNAP, to uncouple AII amacrine cells from cone bipolar cells (cf. Mills & Massey, 1995) and thereby blocking the primary rod pathway to on-center ganglion cells. Likewise, we used the mGluR6 receptor agonist L-AP4 (Bloomfield & Dowling, 1985a, 1985b; Massey, Redburn, & Crawford, 1983; Nakajima et al., 1993; Slaughter & Miller, 1981) to effectively block the responses of rod bipolar cells to block rod-driven signals carried via the primary rod pathway to off-center ganglion cells. Application of either drug had the same overall effect: blockade of the responses of high-sensitivity ganglion cells, but no significant change in the response of intermediate-sensitivity cells (Fig. 4C and D). Taken together, these data indicated that both on- and off-center high-sensitivity ganglion cells received their rod signals via the primary rod pathway. This suggested further that intermediate-sensitivity cells were innervated by the secondary rod pathway. Thus, our results indicated that we could use the scotopic intensity–response function of a ganglion cell to assay the particular pathway that subserved its rod-driven responses.

3.3. Effects of uncoupling AII amacrine cells in the Cx36 knockout mouse

A number of groups have shown that Cx36 forms the gap junctions between AII amacrine cells (Deans et al., 2002; Feigenspan, Teubner, Willecke, & Weiler, 2001; Mills, O'Brien, Li, O'Brien, & Massey, 2001). Therefore, knowing that high-sensitivity ganglion cells are driven by the primary rod pathway, we compared the responses

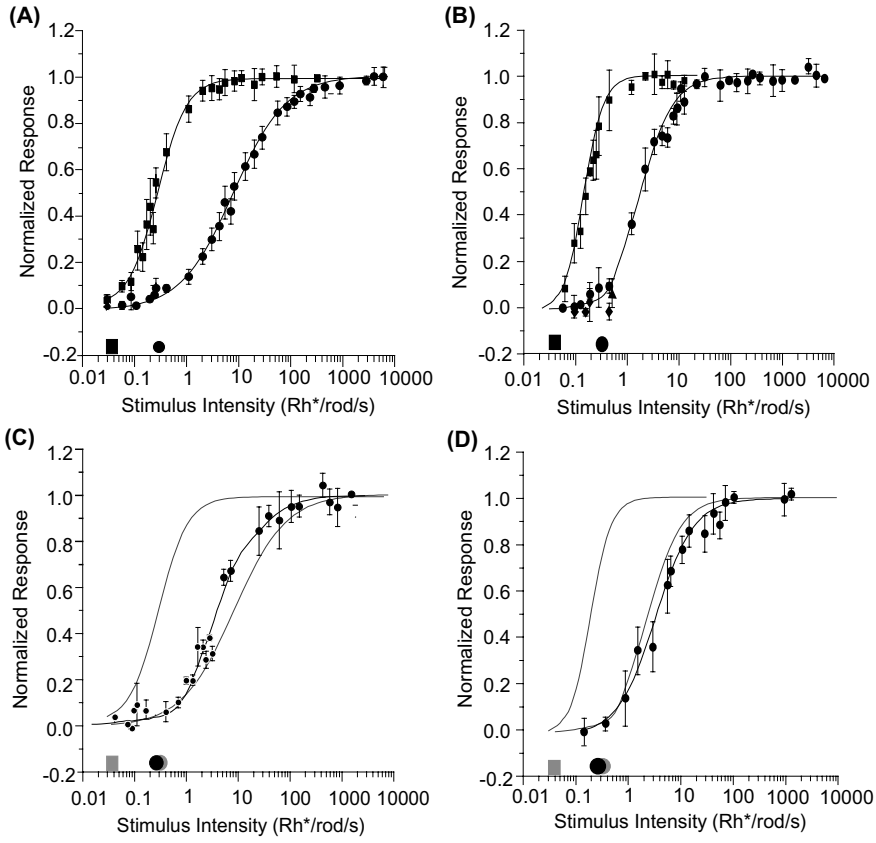

Fig. 4. Normalized responses of on-center (A) and off-center (B) ganglion cells in the wild-type mouse retina presented as a function of light intensity. Each data point shows the average and standard error for a number of cells. The data were fit by Michaelis–Menten equations as described in Section 2. Based on their intensity–response functions under scotopic illumination, ganglion cells could be placed into two groups: high sensitivity (squares) and intermediate sensitivity (circles). Symbols along the abscissa indicate the response thresholds for each class of cell using a 5% of maximum response criterion. (C) Application of 100 μM SNAP abolishes the responses of on-center high-sensitivity ganglion cells, but has no significant effect on responses of on-center intermediate-sensitivity cells. Gray curves indicate intensity–response functions under control conditions. Symbols indicating the thresholds of drug and control data are provided for comparison. (D) Application of 50 μM L-AP4 abolishes the responses of off-center high-sensitivity ganglion cells, but has no significant effect on responses of off-center intermediate-sensitivity cells. Gray curves indicate intensity–response functions under control conditions. Symbols indicating the thresholds of drug and control data are provided for comparison.

of these cells in wild-type and a Cx36 knockout mouse to assay the function of AII–AII cell coupling. We have reported that AII-cone bipolar cell and rod–cone gap junctions are also eliminated in the Cx36 KO mouse retina, thereby blocking both the primary and secondary rod pathway inputs to and the responses of recipient on-center high- and intermediate-sensitivity cells. Therefore, off-center high-sensitivity cells were used to assay the effects of uncoupling AII cells in the Cx36 KO mouse.

Similar to the results with L-AP4 in the wild-type mouse retina, we found that the intensity–response curve corresponding to off-center high-sensitivity cells was abolished in the Cx36 KO mouse, whereas the intermediate-sensitivity cells appeared unaffected in the knockout animal (Fig. 5A). However, the survival of the intermediate-sensitivity OFF cell profile was surprising in that it conflicted with our earlier finding showing that the profile for intermediate-sensitivity on-center cells is lost in the Cx36 knockout mouse (Deans et al., 2002). That is, the loss of on-center intermediate-sensitivity cells reflected the disruption of the secondary rod pathway due to elimination of rod–cone gap junctions. If this was the case, then the responses of both on- and off-center intermediate-sensitivity cells should have been lost in the Cx36 knockout animal. Further, if the surviving off-center cells showing apparent intermediate sensitivity in the knockout mouse were innervated by the secondary rod pathway, then they should not be affected by L-AP4. However, we found this not to be the case. Application of L-AP4 reversibly blocked the responses of the apparent intermediate-sensitivity cells in the Cx36 knockout mice resulting in the complete elimination of both high- and intermediate-sensitivity cell responses (Fig. 5B). These data indicate that the apparent intermediate-sensitivity off-center cells are, in fact, innervated by the primary rod pathway as we found for high-sensitivity cells in wild-type retinas. These data suggest, then, that the apparent intermediate-sensitivity cells in the knockout mouse likely

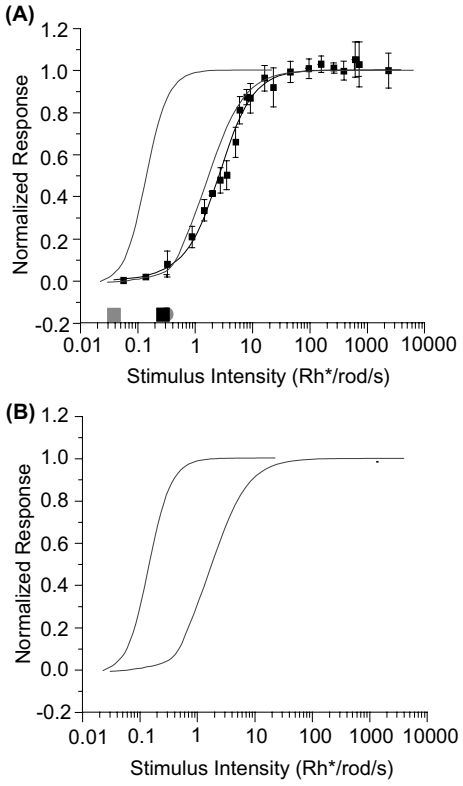

Fig. 5. (A) Comparison of the normalized intensity–response profiles and thresholds of off-center ganglion cells in wild-type (gray curves and symbols) and Cx36 knockout mouse (dark curves and symbols) retinas. Conventions are the same as in Fig. 4. The curve for high-sensitivity cells is missing in the Cx36 knockout retina, whereas the curve for intermediate-sensitivity cells appear to be unaffected. (B) Application of 50 μM L-AP4 reversibly blocked the light-evoked response of the surviving group of cells in the Cx36 KO mouse retina. These data indicate that the apparent intermediate-sensitivity cell is innervated mainly by the primary rod pathway.

correspond to the high-sensitivity cells in control animals, but with rightward shifted intensity–response profiles. Thus, elimination of AII cell coupling in the Cx36 KO mouse resulted in an approximate one log unit loss of sensitivity of the postsynaptic ganglion cells.

4. Discussion

4.1. Function of the light-induced changes in AII cell coupling

Our recent results indicate that the homologous coupling between AII amacrine cells and their resultant receptive field physiology are highly plastic, being modulated under conditions of changing adaptational state. The relationship between coupling and light adaptation followed a curious inverted U-shaped function, in which AII cells were relatively uncoupled in the well dark-adapted retina, show a dramatic increased coupling under the scotopic range and then uncouple again under light-adapted conditions. Converging evidence indicates that the neuromodulator dopamine acts to uncouple AII cells, but it is known to be a light-adapted agent (Witkovsky & Dearry, 1992). Therefore, it remains unclear whether dopamine alone can underlie the uncoupling seen under both light- and dark-adapted conditions.

Whatever the generating mechanisms(s), the important question is: what is the function of the light-induced changes in AII–AII cell coupling? One idea is that these changes reflect the need for AII cells, as vital elements in the rod pathway, to remain responsive throughout the scotopic/mesopic range (Fig. 6). In this scheme, dark adaptation is analogous to starlight conditions under which rods will only sporadically absorb photons of light. The need, then, is for AII cells to preserve these isolated signals above the background noise. Accordingly, the AII cells are relatively uncoupled in that there are few correlated signals to sum; so extensive coupling would serve to dissipate and thereby attenuate the few isolated responses rather than enhance them. Presentation of dim background lights, analogous to twilight conditions, brings about greater than a 10-fold increase in AII–AII cell coupling. This increased coupling provides for summation of synchronous activity over a wider area, thus preserving the fidelity of these rod-driven, correlated signals at the expense of spatial acuity (cf. Smith & Vardi, 1995). This transition in coupling between well dark-adapted retinas and those illuminated with dim background lights suggests two basic operating states for AII cells under scotopic/mesopic light conditions: (1) the ability to respond to single photon events and (2) summing signals over a relatively large area to sum synchronized events above the background noise. Under photopic conditions, coupling between AII cells diminishes to a level similar to that seen under dark adaptation. As detailed below, AII cells also display cone-mediated responses and so the constrained coupling may serve to reduce lateral spread of signals and to thereby preserve high spatial acuity under bright light conditions.

4.2. Function of AII cell coupling

A second important question that we studied was: what is the overall contribution of AII–AII cell coupling to rod signaling in the inner retina? To answer this, we studied high-sensitivity ganglion cells, which are innervated selectively by the primary rod bipolar-AII cell rod pathway, in the Cx36 KO mouse in which the AII cell gap junctions are eliminated. In the Cx36 KO mouse retina, we found that whereas the responses of off-center high-sensitivity cells were eliminated, apparent off-center intermediate-sensitivity cells were unaffected. These data conflict with our previous finding that on-center intermediate-sensitivity cells are

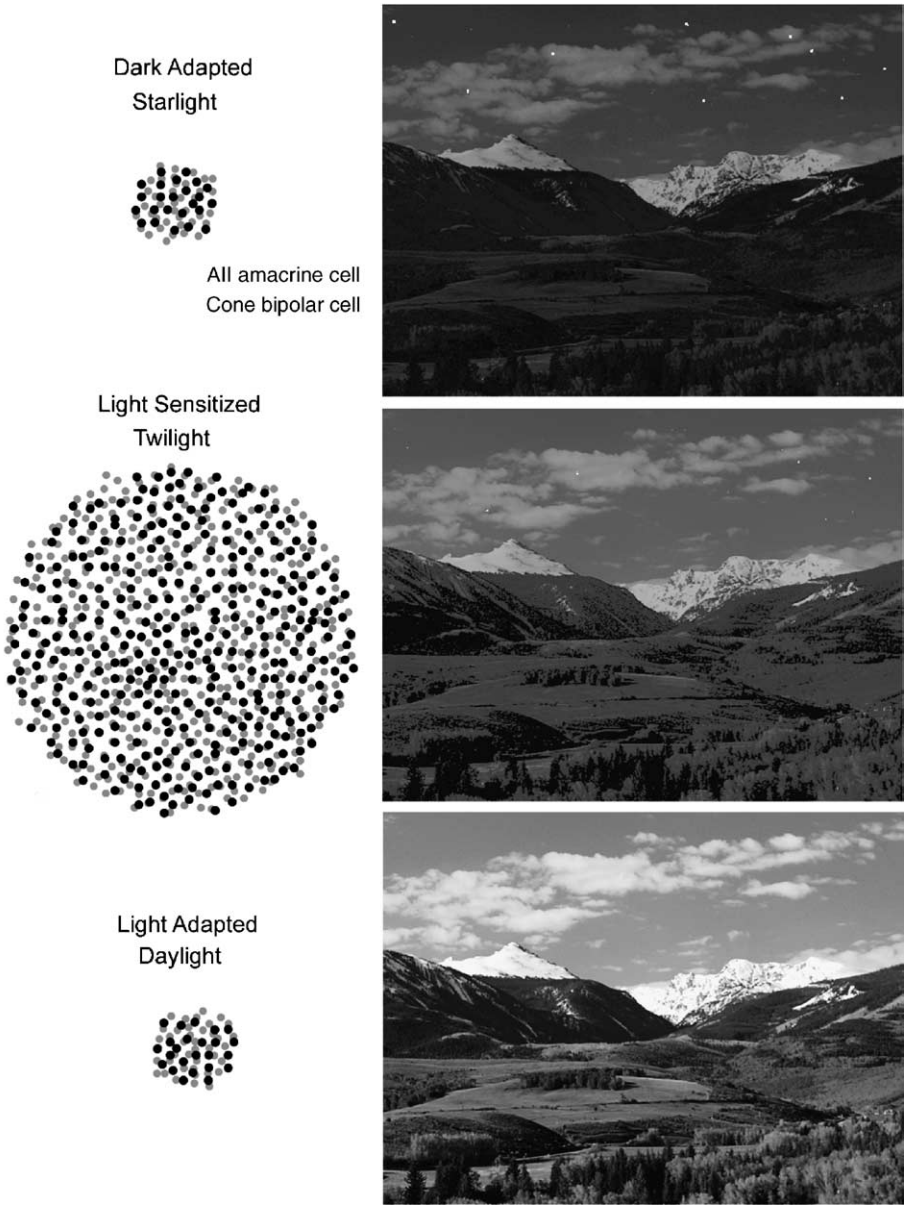

Fig. 6. Diagram illustrating the changes in coupling between AII amacrine cells and between AII cells and on-center cone bipolar cells under different adapting conditions. Cells are relatively uncoupled under dark-adapted conditions (analogous to starlight), but show strong coupling when light sensitized with a dim background light corresponding to twilight. The cells are poorly coupled under light adapted conditions similar to that seen in the dark-adapted state.

missing in the Cx36 knockout retina due to the disruption of rod–cone coupling that is obligatory to the secondary rod pathway (Deans et al., 2002). If so, then responses of intermediate-sensitivity cells should also have been lost if they receive their rod signals through the secondary pathway. However, we found that application of L-AP4 abolished the responses of these apparent intermediate-sensitivity cells. This indicated that they receive rod signals predominantly from the primary and not the secondary rod pathway. Therefore, their physiology appears most consistent with those of high-sensitivity cells. All these data can be reconciled if, as we posit, the apparent intermediate cells in the knockout mouse retina correspond to high-sensitivity–sensitivity cells in wild-type animals, but whose intensity–response profiles are shifted rightward due to a log unit loss of sensitivity.

Based on computational models, Smith and Vardi (1995) speculated that AII cell coupling serves to sum synchronous signals and subtract asynchronous noise thereby preserving the high fidelity of signals carried by the primary rod pathway. Thus, the reduced sensitivity of high-sensitivity cells in the knockout retina likely results from disruption of AII–AII cell coupling and

the resultant reduced signal-to-noise and fidelity of AII cells signals transmitted to off-center ganglion cells. These physiological data are thus consistent with and form the first direct support for the idea that AII–AII cell coupling underlies a unique function of the primary rod pathway: maintaining the high sensitivity of rod signals arriving in the inner retina. In this regard, it is important to note that elimination of AII cell coupling produces a one log unit loss of response sensitivity, exactly the difference seen between high- and intermediate-sensitivity ganglion cells in the wild-type mouse retina.

Acknowledgments

This work was supported by NIH Grant EY07360 to SAB, a Fight for Sight Postdoctoral Fellow (BV), and an unrestricted grant from Research to Prevent Blindness, Inc. We also thank Drs. Daiyan Xin, Michael Deans and David Paul for their contributions to experiments reviewed here.

References

Baylor, D. A., Hodkin, A. L., & Lamb, T. D. (1974). The electrical response of turtle cones to flashes and steps of light. *Journal of Physiology, 242*, 685–727.

Bloomfield, S. A., & Dowling, J. E. (1985a). Roles of aspartate and glutamate in synaptic transmission in rabbit retina. I. Outer plexiform layer. *Journal of Neurophysiology, 53*, 699–713.

Bloomfield, S. A., & Dowling, J. E. (1985b). Roles of aspartate and glutamate in synaptic transmission in rabbit retina. II. Inner plexiform layer. *Journal of Neurophysiology, 53*, 714–725.

Bloomfield, S. A., & Miller, R. F. (1982). A physiological and morphological study of the horizontal cell types in the rabbit retina. *Journal of Comparative Neurology, 208*, 288–303.

Bloomfield, S. A., & Xin, D. (2000). Surround inhibition of mammalian AII amacrine cells is generated in the proximal retina. *Journal of Physiology, 523*, 771–783.

Bloomfield, S. A., Xin, D., & Osborne, T. (1997). Light-induced modulation of coupling between AII amacrine cells in the rabbit retina. *Visual Neuroscience, 14*, 565–576.

Boos, R., Schneider, H., & Wässle, H. (1993). Voltage- and transmitter-gated currents of AII-amacrine cells in a slice preparation of the rat retina. *Journal of Neuroscience, 13*, 2874–2888.

Boycott, B. B., & Dowling, J. E. (1969). Organization of the primate retina: light microscopy. *Philosophical Transactions of the Royal Society B (London), 255*, 109–184.

Boycott, B. B., & Kolb, H. (1973). The connexions between bipolar cells and photoreceptors in the retina of the domestic cat. *Journal of Comparative Neurology, 148*, 115–140.

Boycott, B. B., & Wässle, H. (1991). Morphological classification of bipolar cells in the macaque monkey retina. *European Journal of Neuroscience, 3*, 1069–1088.

Dacheux, R. F., & Raviola, E. (1982). Horizontal cells in the retina of the rabbit. *Journal of Neuroscience, 2*, 1486–1489.

Dacheux, R. F., & Raviola, E. (1986). The rod pathway in the rabbit retina: a depolarizing bipolar and amacrine cell. *Journal of Neuroscience, 6*, 331–345.

Deans, M. R, Gibson, J. R., Sellitto, C., Connors, B. W., & Paul, D. L. (2001). Synchronous activity of inhibitory networks in neocortex requires electrical synapses containing connexin36. *Neuron, 31*, 477–485.

Deans, M. R., Völgyi, B., Goodenough, D. A., Bloomfield, S. A., & Paul, D. L. (2002). Connexin36 is essential for transmission of rod-mediated visual signals in the mammalian retina. *Neuron, 36*, 1–20.

Euler, T., & Wässle, H. (1995). Immunocytochemical identification of cone bipolar cells in the rat retina. *Journal of Comparative Neurology, 361*, 461–478.

Famiglietti, E. V., & Kolb, H. (1975). A bistratified amacrine cell and synaptic circuitry in the inner plexiform layer of the retina. *Brain Research, 84*, 293–300.

Feigenspan, A., Teubner, B., Willecke, K., & Weiler, R. (2001). Expression of neuronal connexin36 in AII amacrine cells of the mammalian retina. *Journal of Neuroscience, 21*, 230–239.

Field, G. D., & Rieke, F. (2002). Mechanisms regulating variability of the single photon responses of mammalian rod photoreceptors. *Neuron, 35*, 733–747.

Hampson, E. C. G. M., Vaney, D. I., & Weiler, R. (1992). Dopaminergic modulation of gap junction permeability between amacrine cells in the mammalian retina. *Journal of Neuroscience, 12*, 4911–4922.

Hu, E. H., Dacheux, R. F., & Bloomfield, S. A. (2000). A flattened retina-eyecup preparation suitable for electrophysiological studies of neurons visualized with trans-scleral infrared illumination. *Journal of Neuroscience Methods, 103*, 209–216.

Jeon, C.-J., Strettoi, E., & Masland, R. H. (1998). The major cell populations of the mouse retina. *Journal of Neuroscience, 18*, 8936–8946.

Kolb, H. (1977). The organization of the outer plexiform layer in the retina of the cat: electron microscopic observations. *Journal of Neurocytology, 6*, 131–153.

Massey, S. C., Redburn, D. A., & Crawford, M. L. J. (1983). The effects of 2-amino-4-phosphonobutyric acid (APB) on the ERG and ganglion cell discharge of rabbit retina. *Vision Research, 23*, 1607–1613.

Mills, S. L., & Massey, S. C. (1995). Differential properties of two gap junctional pathways made by AII amacrine cells. *Nature, 377*, 734–737.

Mills, S. L., O'Brien, J. J., Li, W., O'Brien, J., & Massey, S. C. (2001). Rod pathways in the mammalian retina use connexin36. *Journal of Comparative Neurology, 436*, 336–350.

Naka, K. I., & Rushton, W. A. (1966). An attempt to analyse colour reception by electrophysiology. *Journal of Physiology, 185*, 556–586.

Nakajima, Y., Iwakabe, H., Akazawa, C., Nawa, H., Shigemoto, R., Mizuno, N., et al. (1993). Molecular characterization of a novel metabotropic glutamate receptor mGLUR6 with a high selectivity for L-2-amino-4-phosphono butyrate. *Journal Biological Chemistry, 268*, 11863–11973.

Nelson, R. (1977). Cat cones have rod input: a comparison of response properties of cones and horizontal cell bodies in the retina of the cat. *Journal of Comparative Neurology, 172*, 109–136.

Penn, J. S., & Williams, T. P. (1984). A new microspectrophotometric method for measuring absorbance of rat photoreceptors. *Vision Research, 24*, 1673–1676.

Raviola, E., & Gilula, N. B. (1973). Gap junctions between photo receptor cells in the vertebrate retina. *Proceedings of National Academy of Sciences USA, 70*, 1677–1681.

Schneeweis, D. M., & Schnapf, J. L. (1995). Photovoltages of rods and cones in the macaque retina. *Science, 268*, 1053–1056.

Sharpe, L. T., & Stockman, A. (1999). Rod pathways: the importance of seeing nothing. *Trends in Neuroscience, 22*, 497–504.

Slaughter, M. M., & Miller, R. F. (1981). 2-amino-4-phosphonobutyric acid: a new pharmacological tool for retina research. *Science, 211*, 182–185.

Smith, R. G., & Vardi, N. (1995). Simulation of the AII amacrine cell of mammalian retina: functional consequences of electrical coupling and regenerative membrane properties. *Visual Neuroscience, 12*, 851–860.

Strettoi, E., Dacheux, R. F., & Raviola, E. (1990). Synaptic connections of rod bipolar cells in the inner plexiform layer of the rabbit. *Journal of Comparative Neurology, 295*, 449–466.

Strettoi, E., Dacheux, R. F., & Raviola, E. (1992). Synaptic connections of the narrow-field bistratified rod amacrine cell (AII) in the rabbit retina. *Journal of Comparative Neurology, 325*, 152–168.

Thibos, L. N., & Werblin, F. S. (1978). The properties of surround antagonism elicited by spinning windmill patterns in the mudpuppy retina. *Journal of Physiology, 278*, 101–116.

Vaney, D. I. (1991). Many diverse types of retinal neurons show tracer coupling when injected with biocytin or neurobiotin. *Neuroscience Letters, 125*, 187–190.

Witkovsky, P., & Dearry, A. (1992). Functional roles of dopamine in the vertebrate retina. *Progress in Retinal and Eye Research, 10*, 247–292.